European Journal of Control 63 (2022) 70–81

Contents lists available at ScienceDirect

European Journal of Control

journal homepage: www.elsevier.com/locate/ejcon

Adaptive decentralized Kalman filters with non-common states for nonlinear systems ☆

Vinod K. Saini, Arnab Maity*

Department of Aerospace Engineering, Indian Institute of Technology Bombay, Mumbai 400076, India

ARTICLE INFO

Article history:
Received 9 May 2021
Revised 17 August 2021
Accepted 2 September 2021
Available online 30 September 2021

Recommended by Prof. T Parisini

Keywords:
Decentralized estimation
Adaptive Kalman filter
Fault tolerance
Non-common states

ABSTRACT

This paper presents two fault tolerance methods for decentralized Kalman filter with non-common states (DKF-NCS) for nonlinear systems. The DKF-NCS is used in a sensor network, where states are not uniform across all nodes. To detect and isolate faulty measurements, the χ^2 test has been quite useful, where faulty measurements are detected based on the innovation error and innovation error covariance matrix. However, the innovation error and innovation error covariance matrix are dependent on the predicted state vector and its error covariance along with measurement model. The χ^2 distribution test fails, if the predicted state vector is not consistent with its predicted error covariance matrix. Also, due to processing of set of measurements independently, fault detection happens more often in decentralized estimation compared to centralized estimation. Therefore, discarding the valid measurements based on χ^2 detector may impact the performance of decentralized estimators significantly. To overcome this problem, we propose two adaptive fault tolerance methods. The first method handles faulty measurements at the assimilation step by applying weighted correction of the information and information matrix. The second method modifies the measurement noise matrix based on a closed-form solution, if fault is detected. These methods are validated using 100 simulation runs for a tracking problem. Overall, the proposed methods are demonstrated to be superior compared to the χ^2 test and an existing adaptive extended Kalman filter.

1. Introduction

One of the major advantages of the decentralized Kalman filter (DKF) [8,10,19,27,29] over the centralized Kalman filter (CKF) is that it can handle faults at the individual node and isolate it, whereas in the CKF, individual measurement faults are generally difficult to detect and isolate due to batch processing of the measurements [15]. The χ^2 test [1,15] has been de facto standard to detect and isolate faulty measurements in the CKF and DKF for all practical problems. The χ^2 test works well, if the predicted state vector is consistent with the predicted error covariance matrix (in a sense which is precisely mentioned later in Definition 1). However, the same could be inconsistent, if incorrect control input is used, or incorrect previous state is used to propagate the state vector, or the process modeling is incorrect.

The DKF has a high rate of fault detection due to the handling of measurements of each node independently. Therefore, DKF becomes more vulnerable compared to CKF, if the predicted state vector is not consistent with its error covariance matrix as good measurements are treated as faulty measurements and discarded. Multiple methods have been presented, summarized in Gao et al. [3], Hwang et al. [6] to handle faulty measurements and/or faulty control input, but these methods are limited to the CKF. In this paper, we present two adaptive decentralized Kalman filters for fault detection and isolation. The proposed methods are discussed for a decentralized Kalman filter with non-common states (DKF-NCS) for nonlinear systems [22], represented as adaptive extended decentralized Kalman filter with non-common states (Adaptive EDKF-NCS). The DKF-NCS has been introduced in Saini and Maity [22], Saini et al. [23] to handle non-uniform state vector across nodes of a sensor network. The non-uniformity in the state vector of each node can arise due to heterogeneous sensor dynamics, time-varying sensor biases, or both. Nevertheless, other existing decentralized framework requires the state vector to be the same in order to perform the assimilation step. Hence, redundant states are to be added to the state vector of each node, which in turn increases computational cost. The method proposed in Saini and Maity [22], Saini et al. [23] has addressed this problem without adding redundant states to the state vector of each node as well as compromising on the estimation error performance.

☆ Recommended by T. Parisini.

* Corresponding author.
E-mail addresses: vinod.s@aero.iitb.ac.in (V.K. Saini), arnab@aero.iitb.ac.in (A. Maity).

https://doi.org/10.1016/j.ejcon.2021.09.004
0947-3580/

1.1. Literature survey

In order to determine faulty measurements in a stochastic system, mainly two approaches have been followed in the literature: 1) multiple models based adaptive estimation, where multiple models are considered with different process and measurement noise matrices, and 2) innovation error and its error covariance matrix based adaptive estimation, where adaptive process and measurement noise matrices are considered. The multiple model based methods require significant resources due to the processing of multiple models. Therefore, they are difficult to implement in real-time practical applications due to requirement of significant computational resources onboard. However, they are still used in safety-critical systems. On the other hand, the innovation-based fault detection methods have been extensively used for most of the practical purposes, where safety is not a major concern and computational resources are limited.

Multiple model has been considered in Maybeck [13] to detect faults in sensor and actuator. In [30], the authors have utilized multiple model adaptive methods, presented in Maybeck [13], to detect jamming in a differential GPS-aided inertial system for precision landing application. The adaptive algorithm proposed in Maybeck and Hanlon [14] has been used to diagnose faults in MEMS devices in Izadian [7], and to detect failure in F-16 flight control system under low dynamic pressure condition in Menke and Maybeck [16]. In [12], a selective-reinitialization multiple-model adaptive estimation approach has been presented to improve the performance of multiple-model based approach. In [2], a consistency check has been conducted between the Kalman filter, which estimates the optimal states using all the measurements, and a bank of auxiliary Kalman filters, which process a subset of measurements to detect fault. In [4], the KF residuals have been studied in the presence of unmodeled state transition matrix, input matrix, and output matrix for multiple model adaptive estimators (MMAE). In [5], to detect fault in the flight control system, spectral analysis of the innovations has been performed for MMAE. The above-discussed literature use multiple model approach and have been focused on safety critical applications, e.g. flight control system.

In [15], a fault detection algorithm using the Kalman filter (KF) residuals/innovations has been proposed. This method has used whiteness, mean, and covariance of the innovations to detect fault in the measurements. An innovation based adaptive Kalman filtering has been presented in Mohamed and Schwarz [17], where process and measurement noise matrices are obtained by minimizing the measurement residuals for a time window. This method does not discard any measurements, and uses a history of residuals to obtain an adaptive measurement noise matrix. Since the residuals are computed based on predicted measurements and the actual measurements, the method can compute an inconsistent measurement noise matrix, if the predicted measurements are incorrect. Therefore, instantaneous faulty measurements may affect the performance of the filter. In [31], a residue based detector has been designed for a fully-connected distributed network to detect faulty sensors, where the detector is equivalent to the χ^2 based detector. Each node communicates the innovation/residual with the connected nodes, but the innovation error covariance is based on the history of innovation similar to the method in Mohamed and Schwarz [17]. The residual term is used along with consensus gain term to update the state estimate. The method has solved a faulty residual problem by rejecting faulty node measurements, where faults are introduced during communication. Nevertheless, it does not solve the problem, when the faulty measurements are used in the estimation. In [26], a robust Kalman filter has been presented to handle measurement faults. This robust Kalman filter uses a modified Kalman gain to update the state estimates for a satellite attitude estimation problem. It utilizes the χ^2 test to detect the faulty measurements and the formulation discussed in Mohamed and Schwarz [17] to modify the Kalman gain, if the measurements are detected faulty. Similarly, in [18], the adaptive Kalman filter proposed in Mohamed and Schwarz [17] for centralized Kalman filter has been extended to Kalman consensus filter for a distributed network system to perform consensus. Also, a covariance matching method has been presented to identify faults. In [9], a detection filter has been designed based on Kalman filter philosophy, where active noise cancelling strategy based on reduced measurement residual is adopted to detect a fault in stochastic discrete-time dynamic system. In [25], constraint switching method has been developed in Kalman filter framework to estimate health of a turbofan engine, where the residual matching method, i.e. practical residuals are comparable to theoretical residuals, is used to switch between unconstrained Kalman filter and constrained Kalman filter.

In [28], generalised likelihood ratio test has been used to increase the robustness of a two-stage Kalman filter. In [11] a fast-convergent fault detection and isolation method has been discussed for nonlinear uncertain systems. The presented method identifies faulty control input for linear systems under process model uncertainties. In [20], an optimal strategy has been presented to handle stealthy sensor attack in a networked linear quadratic Gaussian (LQG) system, where the communicated measurement is corrupted to simulate stealthy sensor attack, which in turn affects the state estimation results. Therefore, the LQG optimization problem has been reformulated to handle the stealthy sensor attack problem. In [21], the noise covariance estimation problem has been solved for a linear networked system, where only the measurements of each node are communicated, and due to communication protocol, some of the data are lost. In order to enable the estimator in such cases, an auto-covariance least-square method has been proposed to estimate the measurement noise covariance.

1.2. Contribution

In this paper, two new adaptive fault tolerance methods are presented for a decentralized network. These methods are integrated with the extended decentralized Kalman filter with non-common states for nonlinear systems [22]. The first approach handles the faulty measurements/nodes at the assimilation step by correcting the predicted information and information matrix by a weighting factor α. This weighting factor is computed by the χ^2 test. In the existing literature [31], the factor α is either zero or one based on fault detector, which in fact is considered only for the connecting nodes, i.e., not for the node where the estimation is taking place, and multiplied with the consensus gain term. Also, the existing approach has been presented to solve faulty communication problem by discarding the faulty node. Moreover, in Xia et al. [31], the actual measurements are communicated to the processing node where the estimation takes place, whereas, in this current paper, the information and information matrix are communicated.

The second method modifies the measurement noise matrix at the time of measurement update by a closed-form solution. This method uses instantaneous residuals to obtain adaptive measurement noise matrix. A similar approach has been used in Mohamed and Schwarz [17], where the adaptive measurement noise matrix is obtained by using a history of residuals. Irrespective of presence of fault in the measurements, the residuals have been utilized. Since the residuals are computed based on predicted measurements and the actual measurements, the method can compute an inconsistent measurement noise matrix, if the predicted measurements are in-

correct. Also, the formulation in Mohamed and Schwarz [17] may make the measurement noise matrix correlated.

The proposed methods in this paper use χ^2 detector to detect the faulty measurements, but do not discard them. These methods are integrated with the EDKF-NCS for nonlinear systems and validated for a target tracking problem for three different cases: (1.) no fault, (2.) faulty measurements, and (3.) incorrect initialization. The results of 100 simulation runs show that the proposed adaptive methods perform superior to the χ^2 distribution test in all three cases. To demonstrate their advantages, the proposed methods are also compared with the adaptive Kalman filter method presented in Mohamed and Schwarz [17].

Remark 1. A DKF-NCS has been presented in Saini and Maity [22], Saini et al. [23] and is not an adaptive one. Also, only a part of the first method has been presented in a conference paper [24] for a linear decentralized Kalman filter. In this current paper, the same idea of [24] with the estimation philosophy in Saini and Maity [22] is integrated and extended to nonlinear systems, which is the proposed method 1 defined as the adaptive EDKF-NCS using weighted correction.

1.3. Organization

The paper is divided into four sections. Section 2 presents the decentralized Kalman filter with non-common states for nonlinear systems, represented as extended decentralized Kalman filter with non-common states (EDKF-NCS). In Section 3, two new adaptive extended decentralized Kalman filters with non-common states are proposed. The simulation results are discussed in Section 4 to demonstrate effectiveness of the proposed methods. Section 5 presents the conclusion and the future work of the paper.

2. Extended decentralized Kalman filter with non-common states for nonlinear systems

In this section, the extended decentralized Kalman filter with non-common states for nonlinear systems is presented.

Consider a fully connected network of N nodes represented as a graph $G = (V, E)$, where each node is equipped with a set of sensors. The edge (i, j) is said to exist, if and only if the node i can acquire information from the node j. The neighborhood of the node i is denoted by the set $N_i = \{j \in V \mid (i, j) \in E\}$.

Remark 2. A fully connected network is considered in this paper. Other network topologies are not considered to avoid consensus problem. Studying consensus on a network of non-common states is beyond the scope of this paper and can be considered a possible future research direction. However, the proposed methods can still be used for other network topologies.

Before presenting the proposed EDKF-NCS, the following definition of consistent is given for the sake of completeness.

Definition 1. Consider a random variable vector $\boldsymbol{z}$ with an estimate $\hat{\boldsymbol{z}}$. The estimation error and the associated covariance are given by $\tilde{\boldsymbol{z}} = \boldsymbol{z} - \hat{\boldsymbol{z}}$ and $\boldsymbol{P} = E[(\boldsymbol{z} - \hat{\boldsymbol{z}})(\boldsymbol{z} - \hat{\boldsymbol{z}})^T]$, respectively. Then, the estimated state vector $\hat{\boldsymbol{z}}$, and its error covariance $\boldsymbol{P}$ are said to be consistent for a threshold μ (defined by χ^2 distribution), if

$$\tilde{\boldsymbol{z}}^T \boldsymbol{P}^{-1} \tilde{\boldsymbol{z}} \leq \mu \,.$$

Consider a dynamic nonlinear process model, sensed by ith node, is

$$\boldsymbol{x}_{i,k+1} = f_i(\boldsymbol{x}_{i,k}, \boldsymbol{u}_{i,k}) + \boldsymbol{w}_{i,k} \,, \tag{1}$$

where $\boldsymbol{x}_{i,k} \in \mathbb{R}^{n_i}$ and $\boldsymbol{w}_{i,k} \in \mathbb{R}^{n_i}$ are the state vector and process noise at time instant k, respectively. $f_i : \mathbb{R}^{n_i} \to \mathbb{R}^{n_i}$. $\boldsymbol{x}_{i,k}$ consists of common states $\boldsymbol{x}_k^c \in \mathbb{R}^{n_c}$ and non-common states $\boldsymbol{x}_{i,k}^{nc} \in \mathbb{R}^{n_{nc,i}}$, i.e., $\boldsymbol{x}_{i,k} = [(\boldsymbol{x}_k^c)^T \ (\boldsymbol{x}_{i,k}^{nc})^T]^T$, and $n_i = n_c + n_{nc,i}$. $\boldsymbol{u}_{i,k}$ is control input, which is assumed here as a known variable unless otherwise stated. The common states ($\boldsymbol{x}_k^c$) are observed by all the nodes, whereas non-common states ($\boldsymbol{x}_{i,k}^{nc}$) are node specific.

Let the measurement model of node i at kth time instant be

$$\boldsymbol{z}_{i,k} = h_i(\boldsymbol{x}_{i,k}) + \boldsymbol{v}_{i,k} \,, \tag{2}$$

where $\boldsymbol{z}_{i,k} \in \mathbb{R}^{m_i}$ and $\boldsymbol{v}_{i,k} \in \mathbb{R}^{m_i}$ are the measurement vector and measurement noise of node i at kth time instant, and $h_i : \mathbb{R}^{n_i} \to \mathbb{R}^{m_i}$.

Assumption 1. Functions f_i and h_i in (1) and (2), respectively, are continuously differentiable functions.

Assumption 2. Process noise $\boldsymbol{w}$ and measurement noise $\boldsymbol{v}$ are zero-mean white Gaussian and uncorrelated, i.e.,

$$\mathbb{E}\left[\begin{bmatrix}\boldsymbol{w}_{i,k}\\ \boldsymbol{v}_{i,k}\end{bmatrix}\begin{bmatrix}\boldsymbol{w}_{i,l} & \boldsymbol{v}_{i,l}\end{bmatrix}\right] = \begin{bmatrix}\boldsymbol{Q}_{i,k}\delta_{k,l} & \boldsymbol{0}\\ \boldsymbol{0} & \boldsymbol{R}_{i,k}\delta_{k,l}\end{bmatrix}, \tag{3}$$

where $\boldsymbol{Q}_{i,k} \geq 0$ and $\boldsymbol{R}_{i,k} > 0$ are process noise and measurement noise covariance matrices, and $\delta_{k,l}$ is a Kronecker delta function.

Assumption 3. Measurement noise $\boldsymbol{v}$ of each node is independent with every other node for $\forall\ k, l \geq 0$ and $i, j \in N$, i.e.,

$$\mathbb{E}\left[\begin{bmatrix}\boldsymbol{v}_{i,k}\\ \boldsymbol{v}_{j,k}\end{bmatrix}\begin{bmatrix}\boldsymbol{v}_{i,l} & \boldsymbol{v}_{j,l}\end{bmatrix}\right] = \begin{bmatrix}\boldsymbol{R}_{i,k}\delta_{k,l} & \boldsymbol{0}\\ \boldsymbol{0} & \boldsymbol{R}_{j,k}\delta_{k,l}\end{bmatrix}. \tag{4}$$

Let $\hat{\boldsymbol{x}}_{i,k|k}$ and $\boldsymbol{P}_{i,k|k}$ are the estimated state vector and estimated error covariance matrix, respectively. Also, $\hat{\boldsymbol{x}}_{i,k+1|k}$ and $\boldsymbol{P}_{i,k+1|k}$ are the predicted state vector and predicted error covariance matrix, respectively.

The EDKF-NCS is presented by the following steps.

2.1. Propagation

The previous state estimates and the process model are used to predict the state estimates and error covariance matrix using the equations below, respectively,

$$\hat{\boldsymbol{x}}_{i,k|k-1} = f_i(\hat{\boldsymbol{x}}_{i,k-1|k-1}, \boldsymbol{u}_{i,k}) \,, \tag{5}$$

$$\boldsymbol{P}_{i,k|k-1} = \boldsymbol{A}_{i,k-1}\boldsymbol{P}_{i,k-1|k-1}\boldsymbol{A}_{i,k-1}^T + \boldsymbol{Q}_{i,k-1} \,, \tag{6}$$

where the state transition matrix $\boldsymbol{A}_{i,k-1} \in R^{n_i \times n_i}$ is given by

$$\boldsymbol{A}_{i,k-1} = \frac{\partial f_i}{\partial \boldsymbol{x}_i}(\hat{\boldsymbol{x}}_{i,k-1|k-1}) \,. \tag{7}$$

2.2. Validation

A χ^2 test is conducted on the measurements to detect and isolate faulty measurements. The measurements are considered as faulty measurements for a threshold $\beta_{i,Th}$ (defined by χ^2 distribution) [15], if

$$\beta_{i,k} > \beta_{i,Th} \,, \tag{8}$$

where

$$\beta_{i,k} = \tilde{\boldsymbol{z}}_{i,k}^T \boldsymbol{S}_{i,k}^{-1} \tilde{\boldsymbol{z}}_{i,k} \,, \tag{9}$$

$\tilde{\boldsymbol{z}}_{i,k} = \boldsymbol{z}_{i,k} - \hat{\boldsymbol{z}}_{i,k|k-1}$ is the innovation or measurement residual of ith node, $\hat{\boldsymbol{z}}_{i,k|k-1} = h_i(\hat{\boldsymbol{x}}_{i,k|k-1})$ is the predicted measurement vector, and $\boldsymbol{S}_{i,k} = \boldsymbol{R}_{i,k} + \boldsymbol{H}_{i,k}\boldsymbol{P}_{i,k|k-1}\boldsymbol{H}_{i,k}^T$ is the innovation covariance matrix. The measurement matrix is represented by

$$\boldsymbol{H}_{i,k} = \frac{\partial h_i}{\partial \boldsymbol{x}_i}(\hat{\boldsymbol{x}}_{i,k|k-1}) \,. \tag{10}$$

2.3. Correction

If the measurements are not faulty, the following equations are used to correct the state estimates and the error covariance matrix, respectively,

$$\tilde{\boldsymbol{x}}_{i,k|k} = \hat{\boldsymbol{x}}_{i,k|k-1} + \boldsymbol{K}_{i,k}\left(\boldsymbol{z}_{i,k} - \hat{\boldsymbol{z}}_{i,k|k-1}\right), \tag{11}$$

$$\tilde{\boldsymbol{P}}_{i,k|k} = \left(\boldsymbol{I} - \boldsymbol{K}_{i,k}\boldsymbol{H}_{i,k}\right)\boldsymbol{P}_{i,k|k-1}, \tag{12}$$

where $\boldsymbol{K}_{i,k}$ is Kalman gain, given by

$$\boldsymbol{K}_{i,k} = \boldsymbol{P}_{i,k|k-1}\boldsymbol{H}_{i,k}^T\boldsymbol{S}_{i,k}^{-1}. \tag{13}$$

If the measurements are faulty, the correction equations are not used, instead the predicted state estimates and error covariance matrix become the current state estimates and error covariance matrix, i.e.,

$$\tilde{\boldsymbol{x}}_{i,k|k} = \hat{\boldsymbol{x}}_{i,k|k-1}, \tag{14}$$

$$\tilde{\boldsymbol{P}}_{i,k|k} = \boldsymbol{P}_{i,k|k-1}. \tag{15}$$

2.4. Communication

The common state information $\left(\left(\tilde{\boldsymbol{P}}_{i,k|k}^c\right)^{-1}\tilde{\boldsymbol{x}}_{i,k|k}^c - \left(\boldsymbol{P}_{i,k|k-1}^c\right)^{-1}\hat{\boldsymbol{x}}_{i,k|k-1}^c\right)$ and information matrix $\left(\left(\tilde{\boldsymbol{P}}_{i,k|k}^c\right)^{-1} - \left(\boldsymbol{P}_{i,k|k-1}^c\right)^{-1}\right)$ are shared with connecting nodes.

2.5. Assimilation

The communicated information is used further to correct the state estimates and error covariance matrix using the equations below, respectively,

$$\boldsymbol{P}_{i,k|k}^{-1}\hat{\boldsymbol{x}}_{i,k|k} = \tilde{\boldsymbol{P}}_{i,k|k}^{-1}\tilde{\boldsymbol{x}}_{i,k|k} + \sum_{j\in N_i}\boldsymbol{\Lambda}_{j,k}, \tag{16}$$

$$\boldsymbol{P}_{i,k|k}^{-1} = \tilde{\boldsymbol{P}}_{i,k|k}^{-1} + \sum_{j\in N_i}\bar{\boldsymbol{P}}_{j,k}^{-1}, \tag{17}$$

where

$$\bar{\boldsymbol{P}}_{j,k}^{-1} = \begin{bmatrix} \left(\tilde{\boldsymbol{P}}_{j,k|k}^c\right)^{-1} - \left(\boldsymbol{P}_{j,k|k-1}^c\right)^{-1} & \boldsymbol{0}_{n_c\times n_{nc,i}} \\ \boldsymbol{0}_{n_{nc,i}\times n_c} & \boldsymbol{0}_{n_{nc,i}\times n_{nc,i}} \end{bmatrix},$$

$$\boldsymbol{\Lambda}_{j,k} = \begin{bmatrix} \left(\tilde{\boldsymbol{P}}_{j,k|k}^c\right)^{-1}\tilde{\boldsymbol{x}}_{j,k|k}^c - \left(\boldsymbol{P}_{j,k|k-1}^c\right)^{-1}\hat{\boldsymbol{x}}_{j,k|k-1}^c \\ \boldsymbol{0}_{n_{nc,i}\times 1} \end{bmatrix}.$$

and $\boldsymbol{0}_{n_{nc,i}\times n_c}$ is a zero matrix of order $n_{nc,i}\times n_c$. The EDKF-NCS is summarized in Algorithm 1.

3. Adaptive extended decentralized Kalman filters with non-common states

We propose two new adaptive extended decentralized Kalman filter with non-common states methods in this section. The proposed methods use the χ^2 test to detect faulty measurements. The first method applies weighted correction to information and information matrix at the assimilation step, presented in Section 3.1. The weights are computed based on the χ^2 test. The second method recomputes the measurement noise matrix by a closed-form solution if the measurements fail to pass the χ^2 test, discussed in Section 3.2.

Algorithm 1 EDKF-NCS at ith node.

Initialize: $\hat{\boldsymbol{x}}_{i,0|0}$, $\boldsymbol{P}_{i,0|0}$
while $k \neq k_{end}$ **do**
Propagation:
$\hat{\boldsymbol{x}}_{i,k|k-1} = f_i(\hat{\boldsymbol{x}}_{i,k-1|k-1}, \boldsymbol{u}_{i,k})$; $\boldsymbol{A}_{i,k-1} = \frac{\partial f_i}{\partial \boldsymbol{x}_i}(\hat{\boldsymbol{x}}_{i,k-1|k-1})$
$\boldsymbol{P}_{i,k|k-1} = \boldsymbol{A}_{i,k-1}\boldsymbol{P}_{i,k-1|k-1}\boldsymbol{A}_{i,k-1}^T + \boldsymbol{Q}_{i,k-1}$
Validation:
$\boldsymbol{H}_{i,k} = \frac{\partial h_i}{\partial \boldsymbol{x}_i}(\hat{\boldsymbol{x}}_{i,k|k-1})$; $\boldsymbol{S}_{i,k} = \boldsymbol{R}_{i,k} + \boldsymbol{H}_{i,k}\boldsymbol{P}_{i,k|k-1}\boldsymbol{H}_{i,k}^T$
$\hat{\boldsymbol{z}}_{i,k|k-1} = h_i(\hat{\boldsymbol{x}}_{i,k|k-1})$; $\tilde{\boldsymbol{z}}_{i,k|k-1} = \boldsymbol{z}_{i,k} - \hat{\boldsymbol{z}}_{i,k|k-1}$; $\beta_{i,k} = \tilde{\boldsymbol{z}}_{i,k|k-1}^T\boldsymbol{S}_{i,k}^{-1}\tilde{\boldsymbol{z}}_{i,k|k-1}$
Correction:
if $\beta_{i,k} < \beta_{i,Th}$ **then** $\boldsymbol{K}_{i,k} = \boldsymbol{P}_{i,k|k-1}\boldsymbol{H}_{i,k}^T\boldsymbol{S}_{i,k}^{-1}$
$\tilde{\boldsymbol{P}}_{i,k|k} = \left(\boldsymbol{I} - \boldsymbol{K}_{i,k}\boldsymbol{H}_{i,k}\right)\boldsymbol{P}_{i,k|k-1}$; $\tilde{\boldsymbol{x}}_{i,k|k} = \hat{\boldsymbol{x}}_{i,k|k-1} + \boldsymbol{K}_{i,k}\left(\boldsymbol{z}_{i,k} - \hat{\boldsymbol{z}}_{i,k|k-1}\right)$
else $\tilde{\boldsymbol{P}}_{i,k|k} = \boldsymbol{P}_{i,k|k-1}$; $\tilde{\boldsymbol{x}}_{i,k|k} = \hat{\boldsymbol{x}}_{i,k|k-1}$ **end if**
Communication:
$\left(\tilde{\boldsymbol{P}}_{i,k|k}^c\right)^{-1} - \left(\boldsymbol{P}_{i,k|k-1}^c\right)^{-1}$; $\left(\tilde{\boldsymbol{P}}_{i,k|k}^c\right)^{-1}\tilde{\boldsymbol{x}}_{i,k|k}^c - \left(\boldsymbol{P}_{i,k|k-1}^c\right)^{-1}\hat{\boldsymbol{x}}_{i,k|k-1}^c$
Assimilation:
$\bar{\boldsymbol{P}}_{j,k}^{-1} = \begin{bmatrix} \left(\tilde{\boldsymbol{P}}_{j,k|k}^c\right)^{-1} - \left(\boldsymbol{P}_{j,k|k-1}^c\right)^{-1} & \boldsymbol{0}_{n_c\times n_{nc,i}} \\ \boldsymbol{0}_{n_{nc,i}\times n_c} & \boldsymbol{0}_{n_{nc,i}\times n_{nc,i}} \end{bmatrix}$
$\boldsymbol{\Lambda}_{j,k} = \begin{bmatrix} \left(\tilde{\boldsymbol{P}}_{j,k|k}^c\right)^{-1}\tilde{\boldsymbol{x}}_{j,k|k}^c - \left(\boldsymbol{P}_{j,k|k-1}^c\right)^{-1}\hat{\boldsymbol{x}}_{j,k|k-1}^c \\ \boldsymbol{0}_{n_{nc,i}\times 1} \end{bmatrix}$
$\boldsymbol{P}_{i,k|k}^{-1} = \tilde{\boldsymbol{P}}_{i,k|k}^{-1} + \sum_{j\in N_i}\bar{\boldsymbol{P}}_{j,k}^{-1}$; $\boldsymbol{P}_{i,k|k}^{-1}\hat{\boldsymbol{x}}_{i,k|k} = \tilde{\boldsymbol{P}}_{i,k|k}^{-1}\tilde{\boldsymbol{x}}_{i,k|k} + \sum_{j\in N_i}\boldsymbol{\Lambda}_{j,k}$
end while

3.1. Adaptive EDKF-NCS using weighted correction

In this subsection, an adaptive extended decentralized Kalman filter is presented using Theorem 1, where each node is assigned with a weight based on the χ^2 test.

Theorem 1. *Consider the process model and measurement model of node i represented by (1) and (2), respectively. Then the assimilation step at node i is given by*

$$\boldsymbol{P}_{i,k|k}^{-1}\hat{\boldsymbol{x}}_{i,k|k} = \left(1-\alpha_{i,k}\right)\boldsymbol{P}_{i,k|k-1}^{-1}\hat{\boldsymbol{x}}_{i,k|k-1} + \alpha_{i,k}\tilde{\boldsymbol{P}}_{i,k|k}^{-1}\tilde{\boldsymbol{x}}_{i,k|k} + \sum_{j\in N_i}\alpha_{j,k}\boldsymbol{\Lambda}_{j,k}, \tag{18}$$

$$\boldsymbol{P}_{i,k|k}^{-1} = \left(1-\alpha_{i,k}\right)\boldsymbol{P}_{i,k|k-1}^{-1} + \alpha_{i,k}\tilde{\boldsymbol{P}}_{i,k|k}^{-1} + \sum_{j\in N_i}\alpha_{j,k}\bar{\boldsymbol{P}}_{j,k}^{-1}, \tag{19}$$

where

$$\alpha_{i,k} = \begin{cases} \frac{\beta_{i,Th}}{\beta_{i,k}}, & \text{if } \beta_{i,k} > \beta_{i,Th} \\ 1, & otherwise. \end{cases} \tag{20}$$

Proof. From the assimilation step, (16) can be written as

$$\boldsymbol{P}_{i,k|k}^{-1}\hat{\boldsymbol{x}}_{i,k|k} = \boldsymbol{P}_{i,k|k-1}^{-1}\hat{\boldsymbol{x}}_{i,k|k-1} + \left(\tilde{\boldsymbol{P}}_{i,k|k}^{-1}\tilde{\boldsymbol{x}}_{i,k|k} - \boldsymbol{P}_{i,k|k-1}^{-1}\hat{\boldsymbol{x}}_{i,k|k-1}\right) + \sum_{j\in N_i}\boldsymbol{\Lambda}_{j,k}. \tag{21}$$

Also, (17) can be expressed as

$$\boldsymbol{P}_{i,k|k}^{-1} = \boldsymbol{P}_{i,k|k-1}^{-1} + \left(\tilde{\boldsymbol{P}}_{i,k|k}^{-1} - \boldsymbol{P}_{i,k|k-1}^{-1}\right) + \sum_{j\in N_i}\bar{\boldsymbol{P}}_{j,k}^{-1}. \tag{22}$$

From the above equations, it is evident that the assimilation equations involve predicted information $\left(\boldsymbol{P}_{i,k|k-1}^{-1}\hat{\boldsymbol{x}}_{i,k|k-1}\right)$ and predicted information matrix $\left(\boldsymbol{P}_{i,k|k-1}^{-1}\right)$ of a node based on the process

model, and the corrected information $\left(\tilde{\boldsymbol{P}}^{-1}_{i,k|k}\tilde{\boldsymbol{x}}_{i,k|k} - \boldsymbol{P}^{-1}_{i,k|k-1}\hat{\boldsymbol{x}}_{i,k|k-1}\right)$ and corrected information matrix $\left(\tilde{\boldsymbol{P}}^{-1}_{i,k|k} - \boldsymbol{P}^{-1}_{i,k|k-1}\right)$ of the node, and the common corrected information, represented as $\left(\left(\tilde{\boldsymbol{P}}^{c}_{j,k|k}\right)^{-1}\tilde{\boldsymbol{x}}^{c}_{j,k|k} - \left(\boldsymbol{P}^{c}_{j,k|k-1}\right)^{-1}\tilde{\boldsymbol{x}}^{c}_{j,k|k-1}\right)$ and common corrected information matrix, represented as $\left(\left(\tilde{\boldsymbol{P}}^{c}_{j,k|k}\right)^{-1} - \left(\boldsymbol{P}^{c}_{j,k|k-1}\right)^{-1}\right)$ present in $\boldsymbol{\Lambda}_{j,k}$ and $\bar{\boldsymbol{P}}^{-1}_{j,k}$ of the connecting nodes, respectively.

In order to handle faulty nodes, we assign a weight $\alpha_{i,k}$ to the corrections of each node. Thus, the assimilation equations become

$$\boldsymbol{P}^{-1}_{i,k|k}\hat{\boldsymbol{x}}_{i,k|k} = \boldsymbol{P}^{-1}_{i,k|k-1}\hat{\boldsymbol{x}}_{i,k|k-1} \tag{23}$$

$$+\alpha_i\left(\tilde{\boldsymbol{P}}^{-1}_{i,k|k}\tilde{\boldsymbol{x}}_{i,k|k} - \boldsymbol{P}^{-1}_{i,k|k-1}\hat{\boldsymbol{x}}_{i,k|k-1}\right) + \sum_{j\in N_i}\alpha_j\boldsymbol{\Lambda}_{j,k}\,, \tag{23}$$

$$\boldsymbol{P}^{-1}_{i,k|k} = \boldsymbol{P}^{-1}_{i,k|k-1} + \alpha_i\left(\tilde{\boldsymbol{P}}^{-1}_{i,k|k} - \boldsymbol{P}^{-1}_{i,k|k-1}\right) + \sum_{j\in N_i}\alpha_j\bar{\boldsymbol{P}}^{-1}_{j,k}. \tag{24}$$

We compute $\alpha_{i,k}$ based on the χ^2 test. For a valid node (i.e., $\beta_{i,k} \le \beta_{i,Th}$), $\alpha_{i,k} = 1$. For a faulty node, it is defined by

$$\alpha_{i,k} = \frac{\beta_{i,Th}}{\beta_{i,k}}\,. \tag{25}$$

Note that, for a faulty node, $\beta_{i,k} > \beta_{i,Th}$, therefore $\alpha_{i,k} < 1$. Hence, less weightage is given to the corrections from a faulty node. Solving the above equations further, we get

$$\boldsymbol{P}^{-1}_{i,k|k}\hat{\boldsymbol{x}}_{i,k|k} = \left(1-\alpha_{i,k}\right)\boldsymbol{P}^{-1}_{i,k|k-1}\hat{\boldsymbol{x}}_{i,k|k-1} + \alpha_{i,k}\tilde{\boldsymbol{P}}^{-1}_{i,k|k}\tilde{\boldsymbol{x}}_{i,k|k} + \sum_{j\in N_i}\alpha_{j,k}\boldsymbol{\Lambda}_{j,k}, \tag{26}$$

$$\boldsymbol{P}^{-1}_{i,k|k} = \left(1-\alpha_{i,k}\right)\boldsymbol{P}^{-1}_{i,k|k-1} + \alpha_{i,k}\tilde{\boldsymbol{P}}^{-1}_{i,k|k} + \sum_{j\in N_i}\alpha_{j,k}\bar{\boldsymbol{P}}^{-1}_{j,k}\,. \tag{27}$$

□

The proposed weighted correction based adaptive EDKF-NCS is summarized in Algorithm 2.

3.2. Adaptive EDKF-NCS using measurement noise matrix modification

An adaptive EDKF-NCS based on measurement noise matrix modification is proposed here. In this proposed approach, a closed-form solution is presented to re-compute measurement noise matrix of a faulty node.

In the EDKF-NCS, the χ^2 test is used to detect and isolate faulty measurements. However, instead of discarding the faulty measurements, measurement noise matrix is re-computed in the proposed adaptive EDKF-NCS. The similar approach was proposed by Mohamed and Schwarz [17], where process and measurement noise covariance matrices, $\boldsymbol{Q}$ and $\boldsymbol{R}$ respectively, are computed based on innovation and innovation error covariance. However, it uses the history of innovation to estimate $\boldsymbol{Q}$ and $\boldsymbol{R}$ in real-time. But, in the proposed method in this subsection, $\boldsymbol{R}$ matrix is updated using a closed-form solution.

Theorem 2. *Consider the process model and measurement model of a dynamic stochastic system given by (1) and (2), respectively. Then the measurement noise matrix $\boldsymbol{R}_{i,k}$, used in decentralized estimation, of a faulty node i at kth time instant is computed as*

$$\boldsymbol{R}^{new}_{i,k} = \left(\frac{\beta_{i,k}}{\beta_{i,Th}}\right)\boldsymbol{R}_{i,k} + \left(\frac{\beta_{i,k}}{\beta_{i,Th}} - 1\right)\boldsymbol{H}_{i,k}\boldsymbol{P}_{i,k|k-1}\boldsymbol{H}^T_{i,k}\,, \tag{28}$$

where the node i is considered as faulty, if $\beta_{i,k} > \beta_{i,Th}$.

Algorithm 2 Adaptive EDKF-NCS using weighted correction at ith node.

Initialize: $\hat{\boldsymbol{x}}_{i,0|0}$, $\boldsymbol{P}_{i,0|0}$
while $k \neq k_{end}$ **do**
Propagation:
$\hat{\boldsymbol{x}}_{i,k|k-1} = f_i(\hat{\boldsymbol{x}}_{i,k-1|k-1}, \boldsymbol{u}_{i,k})$; $\boldsymbol{A}_{i,k-1} = \frac{\partial f_i}{\partial \boldsymbol{x}_i}(\hat{\boldsymbol{x}}_{i,k-1|k-1})$
$\boldsymbol{P}_{i,k|k-1} = \boldsymbol{A}_{i,k-1}\boldsymbol{P}_{i,k-1|k-1}\boldsymbol{A}^T_{i,k-1} + \boldsymbol{Q}_{i,k-1}$
Validation:
$\boldsymbol{H}_{i,k} = \frac{\partial h_i}{\partial \boldsymbol{x}_i}(\hat{\boldsymbol{x}}_{i,k|k-1})$; $\boldsymbol{S}_{i,k} = \boldsymbol{R}_{i,k} + \boldsymbol{H}_{i,k}\boldsymbol{P}_{i,k|k-1}\boldsymbol{H}^T_{i,k}$
$\hat{\boldsymbol{z}}_{i,k|k-1} = h_i(\hat{\boldsymbol{x}}_{i,k|k-1})$; $\tilde{\boldsymbol{z}}_{i,k|k-1} = \boldsymbol{z}_{i,k} - \hat{\boldsymbol{z}}_{i,k|k-1}$; $\beta_{i,k} = \tilde{\boldsymbol{z}}^T_{i,k|k-1}\boldsymbol{S}^{-1}_{i,k}\tilde{\boldsymbol{z}}_{i,k|k-1}$
if $\beta_{i,k} > \beta_{i,Th}$ **then** $\alpha_{i,k} = \frac{\beta_{i,Th}}{\beta_{i,k}}$ **else** $\alpha_{i,k} = 1$ **end if**
Correction:
$\boldsymbol{K}_{i,k} = \boldsymbol{P}_{i,k|k-1}\boldsymbol{H}^T_{i,k}\boldsymbol{S}^{-1}_{i,k}$; $\tilde{\boldsymbol{P}}_{i,k|k} = \left(\boldsymbol{I} - \boldsymbol{K}_{i,k}\boldsymbol{H}_{i,k}\right)\boldsymbol{P}_{i,k|k-1}$
$\tilde{\boldsymbol{x}}_{i,k|k} = \hat{\boldsymbol{x}}_{i,k|k-1} + \boldsymbol{K}_{i,k}\left(\boldsymbol{z}_{i,k} - \hat{\boldsymbol{z}}_{i,k|k-1}\right)$
Communication:
$\left(\tilde{\boldsymbol{P}}^{c}_{i,k|k}\right)^{-1} - \left(\boldsymbol{P}^{c}_{i,k|k-1}\right)^{-1}$; $\left(\tilde{\boldsymbol{P}}^{c}_{i,k|k}\right)^{-1}\tilde{\boldsymbol{x}}^{c}_{i,k|k} - \left(\boldsymbol{P}^{c}_{i,k|k-1}\right)^{-1}\hat{\boldsymbol{x}}^{c}_{i,k|k-1}$; $\alpha_{i,k}$
Assimilation:
$\bar{\boldsymbol{P}}^{-1}_{j,k} = \begin{bmatrix}\left(\tilde{\boldsymbol{P}}^{c}_{j,k|k}\right)^{-1} - \left(\boldsymbol{P}^{c}_{j,k|k-1}\right)^{-1} & \boldsymbol{0}_{n_c\times n_{nc,i}}\\ \boldsymbol{0}_{n_{nc,i}\times n_c} & \boldsymbol{0}_{n_{nc,i}\times n_{nc,i}}\end{bmatrix}$
$\boldsymbol{\Lambda}_{j,k} = \begin{bmatrix}\left(\tilde{\boldsymbol{P}}^{c}_{j,k|k}\right)^{-1}\tilde{\boldsymbol{x}}^{c}_{j,k|k} - \left(\boldsymbol{P}^{c}_{j,k|k-1}\right)^{-1}\hat{\boldsymbol{x}}^{c}_{j,k|k-1}\\ \boldsymbol{0}_{n_{nc,i}\times 1}\end{bmatrix}$
$\boldsymbol{P}^{-1}_{i,k|k} = \left(1-\alpha_{i,k}\right)\boldsymbol{P}^{-1}_{i,k|k-1} + \alpha_{i,k}\tilde{\boldsymbol{P}}^{-1}_{i,k|k} + \sum_{j\in N_i}\alpha_{j,k}\bar{\boldsymbol{P}}^{-1}_{j,k}$
$\boldsymbol{P}^{-1}_{i,k|k}\hat{\boldsymbol{x}}_{i,k|k} = \left(1-\alpha_{i,k}\right)\boldsymbol{P}^{-1}_{i,k|k-1}\hat{\boldsymbol{x}}_{i,k|k-1} + \alpha_{i,k}\tilde{\boldsymbol{P}}^{-1}_{i,k|k}\tilde{\boldsymbol{x}}_{i,k|k} + \sum_{j\in N_i}\alpha_{j,k}\boldsymbol{\Lambda}_{j,k}$
end while

Proof. Using (9), the χ^2 test of measurement $\boldsymbol{z}_{i,k|k}$ is given as

$$\beta_{i,k} = \tilde{\boldsymbol{z}}^T_{i,k|k-1}\boldsymbol{S}^{-1}_{i,k}\tilde{\boldsymbol{z}}_{i,k|k-1} = \tilde{\boldsymbol{z}}^T_{i,k|k-1}\left(\boldsymbol{R}_{i,k} + \boldsymbol{H}_{i,k}\boldsymbol{P}_{i,k|k-1}\boldsymbol{H}^T_{i,k}\right)^{-1}\tilde{\boldsymbol{z}}_{i,k|k-1}\,, \tag{29}$$

where $\tilde{\boldsymbol{z}}_{i,k} = \boldsymbol{z}_{i,k} - \hat{\boldsymbol{z}}_{i,k|k-1}$. We compare $\beta_{i,k}$ with a threshold $\beta_{i,Th}$ to detect any fault in the measurement, i.e., if $\beta_{i,k} > \beta_{i,Th}$, the measurement is faulty. In order to satisfy $\beta_{i,k}$ within the bound, we update the measurement noise matrix. Let us assume that, for measurement noise covariance matrix $\boldsymbol{R}^{new}_{i,k}$, $\beta_{i,k} = \beta_{i,Th}$. Therefore, (29) can be written as

$$\beta_{i,Th} = \tilde{\boldsymbol{z}}^T_{i,k|k-1}\left(\boldsymbol{R}^{new}_{i,k} + \boldsymbol{H}_{i,k}\boldsymbol{P}_{i,k|k-1}\boldsymbol{H}^T_{i,k}\right)^{-1}\tilde{\boldsymbol{z}}_{i,k|k-1}\,. \tag{30}$$

Using (29) and (30), the following can be expressed as

$$\tilde{\boldsymbol{z}}^T_{i,k|k-1}\Big(\beta_{i,k}\left(\boldsymbol{R}^{new}_{i,k} + \boldsymbol{H}_{i,k}\boldsymbol{P}_{i,k|k-1}\boldsymbol{H}^T_{i,k}\right)^{-1} - \beta_{i,Th}\left(\boldsymbol{R}_{i,k} + \boldsymbol{H}_{i,k}\boldsymbol{P}_{i,k|k-1}\boldsymbol{H}^T_{i,k}\right)^{-1}\Big)\tilde{\boldsymbol{z}}_{i,k|k-1} = 0\,. \tag{31}$$

Since $\tilde{\boldsymbol{z}}^T_{i,k|k-1} \neq \boldsymbol{0}_{m_i\times 1}$, $\forall\tilde{\boldsymbol{z}}^T_{i,k|k-1} \in \mathbb{R}^{m_i}$, it can be written from (31) as

$$\beta_{i,k}\left(\boldsymbol{R}^{new}_{i,k} + \boldsymbol{H}_{i,k}\boldsymbol{P}_{i,k|k-1}\boldsymbol{H}^T_{i,k}\right)^{-1} - \beta_{i,Th}\left(\boldsymbol{R}_{i,k} + \boldsymbol{H}_{i,k}\boldsymbol{P}_{i,k|k-1}\boldsymbol{H}^T_{i,k}\right)^{-1} = 0, \tag{32}$$

which can be further expressed as

$$\left(\boldsymbol{R}^{new}_{i,k} + \boldsymbol{H}_{i,k}\boldsymbol{P}_{i,k|k-1}\boldsymbol{H}^T_{i,k}\right) - \frac{\beta_{i,k}}{\beta_{i,Th}}\left(\boldsymbol{R}_{i,k} + \boldsymbol{H}_{i,k}\boldsymbol{P}_{i,k|k-1}\boldsymbol{H}^T_{i,k}\right) = 0\,. \tag{33}$$

From (33), $\boldsymbol{R}^{new}_{i,k}$ can be derived as

$$\boldsymbol{R}^{new}_{i,k} = \left(\frac{\beta_{i,k}}{\beta_{i,Th}}\right)\boldsymbol{R}_{i,k} + \left(\frac{\beta_{i,k}}{\beta_{i,Th}} - 1\right)\boldsymbol{H}_{i,k}\boldsymbol{P}_{i,k|k-1}\boldsymbol{H}^T_{i,k}\,. \tag{34}$$

As we know $\beta_{i,k} > \beta_{i,Th}$, we have $\boldsymbol{R}_{i,k}^{new} > \boldsymbol{R}_{i,k}$ for a faulty measurement. □

In Algorithm 3, the proposed EDKF-NCS based on adaptive measurement noise matrix is summarized.

Algorithm 3 Adaptive EDKF-NCS using measurement noise matrix modification at ith node.

Initialize: $\hat{\boldsymbol{x}}_{i,0|0}$, $\boldsymbol{P}_{i,0|0}$
while $k \neq k_{end}$ **do**
Propagation:
$\hat{\boldsymbol{x}}_{i,k|k-1} = f_i(\hat{\boldsymbol{x}}_{i,k-1|k-1}, \boldsymbol{u}_{i,k})$; $\boldsymbol{A}_{i,k-1} = \frac{\partial f_i}{\partial \boldsymbol{x}_i}(\hat{\boldsymbol{x}}_{i,k-1|k-1})$
$\boldsymbol{P}_{i,k|k-1} = \boldsymbol{A}_{i,k-1}\boldsymbol{P}_{i,k-1|k-1}\boldsymbol{A}_{i,k-1}^T + \boldsymbol{Q}_{i,k-1}$
Validation:
$\boldsymbol{H}_{i,k} = \frac{\partial h_i}{\partial \boldsymbol{x}_i}(\hat{\boldsymbol{x}}_{i,k|k-1})$; $\boldsymbol{S}_{i,k} = \boldsymbol{R}_{i,k} + \boldsymbol{H}_{i,k}\boldsymbol{P}_{i,k|k-1}\boldsymbol{H}_{i,k}^T$
$\hat{\boldsymbol{z}}_{i,k|k-1} = h_i(\hat{\boldsymbol{x}}_{i,k|k-1})$
$\tilde{\boldsymbol{z}}_{i,k|k-1} = \boldsymbol{z}_{i,k} - \hat{\boldsymbol{z}}_{i,k|k-1}$; $\beta_{i,k} = \tilde{\boldsymbol{z}}_{i,k|k-1}^T \boldsymbol{S}_{i,k}^{-1} \tilde{\boldsymbol{z}}_{i,k|k-1}$
if $\beta_{i,k+1} > \beta_{i,Th}$ **then** $\boldsymbol{R}_{i,k} = \frac{\beta_{i,k}}{\beta_{i,Th}}\boldsymbol{R}_{i,k} + (\frac{\beta_{i,k}}{\beta_{i,Th}} - 1)\boldsymbol{H}_{i,k}\boldsymbol{P}_{i,k|k-1}\boldsymbol{H}_{i,k}^T$
$\boldsymbol{S}_{i,k} = \boldsymbol{R}_{i,k} + \boldsymbol{H}_{i,k}\boldsymbol{P}_{i,k|k-1}\boldsymbol{H}_{i,k}^T$**end if**
Correction:
$\boldsymbol{K}_{i,k} = \boldsymbol{P}_{i,k|k-1}\boldsymbol{H}_{i,k}^T\boldsymbol{S}_{i,k}^{-1}$; $\tilde{\boldsymbol{P}}_{i,k|k} = \big(\boldsymbol{I} - \boldsymbol{K}_{i,k}\boldsymbol{H}_{i,k}\big)\boldsymbol{P}_{i,k|k-1}$
$\tilde{\boldsymbol{x}}_{i,k|k} = \hat{\boldsymbol{x}}_{i,k|k-1} + \boldsymbol{K}_{i,k}\big[\boldsymbol{z}_{i,k} - \hat{\boldsymbol{z}}_{i,k|k-1}\big]$
Communication:
$\Big(\tilde{\boldsymbol{P}}_{i,k|k}^c\Big)^{-1} - \big(\boldsymbol{P}_{i,k|k-1}^c\big)^{-1}, \Big(\tilde{\boldsymbol{P}}_{i,k|k}^c\Big)^{-1}\tilde{\boldsymbol{x}}_{i,k|k}^c - \big(\boldsymbol{P}_{i,k|k-1}^c\big)^{-1}\hat{\boldsymbol{x}}_{i,k|k-1}^c$
Assimilation:
$$\bar{\boldsymbol{P}}_{j,k}^{-1} = \begin{bmatrix} \Big(\tilde{\boldsymbol{P}}_{j,k|k}^c\Big)^{-1} - \big(\boldsymbol{P}_{j,k|k-1}^c\big)^{-1} & \boldsymbol{0}_{n_c \times n_{nc,i}} \\ \boldsymbol{0}_{n_{nc,i} \times n_c} & \boldsymbol{0}_{n_{nc,i} \times n_{nc,i}} \end{bmatrix}$$
$$\boldsymbol{\Lambda}_{j,k} = \begin{bmatrix} \Big(\tilde{\boldsymbol{P}}_{j,k|k}^c\Big)^{-1}\tilde{\boldsymbol{x}}_{j,k|k}^c - \big(\boldsymbol{P}_{j,k|k-1}^c\big)^{-1}\hat{\boldsymbol{x}}_{j,k|k-1}^c \\ \boldsymbol{0}_{n_{nc,i} \times 1} \end{bmatrix}$$
$\boldsymbol{P}_{i,k|k}^{-1} = \tilde{\boldsymbol{P}}_{i,k|k}^{-1} + \sum_{j \in N_i} \bar{\boldsymbol{P}}_{j,k}^{-1}$; $\boldsymbol{P}_{i,k|k}^{-1}\hat{\boldsymbol{x}}_{i,k|k} = \tilde{\boldsymbol{P}}_{i,k|k}^{-1}\tilde{\boldsymbol{x}}_{i,k|k} + \sum_{j \in N_i} \boldsymbol{\Lambda}_{j,k}$
end while

Remark 3. According to (34), the updated measurement noise matrix may not be diagonal due to $\boldsymbol{H}_{i,k}\boldsymbol{P}_{i,k|k-1}\boldsymbol{H}_{i,k}^T$ term, i.e., in case if measurements of a node are uncorrelated, the presented approach could make the measurements correlated. The better approach to update measurement noise matrix, in the case of uncorrelated measurements, would be

$$\boldsymbol{R}_{i,k}^{new} = \left(\frac{\beta_{i,k}}{\beta_{i,Th}}\right)\boldsymbol{R}_{i,k} + \left(\frac{\beta_{i,k}}{\beta_{i,Th}} - 1\right)\boldsymbol{\Gamma}_{i,k}, \tag{35}$$

where $\boldsymbol{\Gamma}_{i,k}$ is a diagonal matrix such that $\boldsymbol{\Gamma}_{i,k} - \boldsymbol{H}_{i,k}\boldsymbol{P}_{i,k|k-1}\boldsymbol{H}_{i,k}^T \geq 0$.

Remark 4. The χ^2 test method uses predicted state vector and predicted error covariance to detect fault in measurements. The method works fine if the predicted state vector is consistent with the predicted error covariance matrix or in other words the predicted measurement vector is consistent with the predicted measurement error covariance defined by the innovation covariance matrix $\boldsymbol{S}_{i,k}$. The method discards measurements if they are found faulty. The disadvantage of discarding the measurement is that if the predicted measurements are incorrect, the valid measurements are discarded and not used in the correction step. Therefore, the state estimates diverge from the true values or take time to converge. This problem occurs more frequent in DKF than CKF due to high fault detection rate in DKF. With the proposed methods, the state estimates can still converge to true values, as it does not discard the measurements, instead use them with lesser weights. Though, the convergence may be slower due to the less weightage to the corrections of inconsistent measurements.

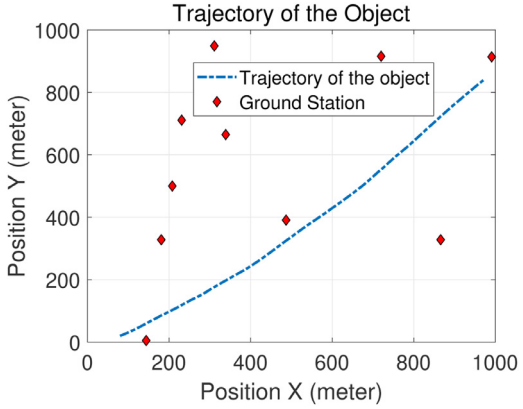

Fig. 1. Truth trajectory of the object.

Remark 5. The main difference between Algorithms 2 and 3 is the communication cost. Algorithm 2 needs to communicate $\alpha_{j,k}$ with the other nodes and handles the faulty measurements at assimilation step, whereas Algorithm 3 does not require additional communication cost.

4. Simulation results and discussions

In this section, simulation results are presented for the proposed adaptive EDKF-NCS methods discussed in Section 3. In Section 4.1, the process model of each node is described. In Section 4.2, the measurement model is presented. The augmentation of additional states in the process model due to bias in the measurements is explained in Section 4.3. Section 4.4 provides results of 100 simulation runs of the proposed methods and comparisons with the χ^2 distribution test and an adaptive extended Kalman filter (AEKF) [17] for three different cases.

A 2D target tracking problem is simulated, where 10 ground stations represented as nodes are tracking an object. Each ground station is equipped with sensors to measure range, range rate, and azimuth angle. All the ground stations are connected with each other and capable to communicate information and information matrix of the common states (position and velocity states) of the target. The true trajectory of the object and the positions of the ground stations are shown in Fig. 1.

4.1. Process model

A zero-mean white noise acceleration model is considered to capture the dynamics of the object as

$$\dot{p}_{x,k} = v_{x,k}, \quad \dot{p}_{y,k} = v_{y,k}, \quad \dot{v}_{x,k} = \tilde{w}_x, \quad \dot{v}_{y,k} = \tilde{w}_y, \tag{36}$$

where $p_{x,k}$ and $p_{y,k}$ are the positions, $v_{x,k}$ and $v_{y,k}$ are the velocities in the x-axis and the y-axis directions at time instant k. $\tilde{w}_x$ and $\tilde{w}_y$ are white Gaussian noises having power spectral densities (PSDs) η_x and η_y, respectively.

4.2. Measurement model

Each ground station consists of range, azimuth, and range rate sensors. The range and azimuth are affected by white Gaussian noises, whereas range rate is affected by time varying bias along with white Gaussian noise. The range measurement at ith ground station is given by

$$r_{i,k} = \sqrt{(p_{x,k} - p_{x,gs_i})^2 + (p_{y,k} - p_{y,gs_i})^2} + v_{r_i}, \tag{37}$$

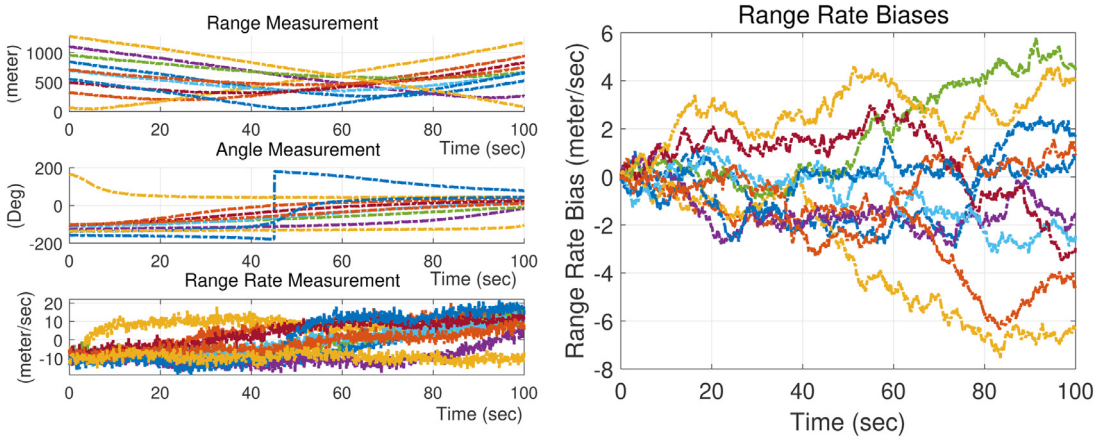

(a) Measurements (b) Range Rate Bias

Fig. 2. Sensor measurements.

the azimuth angle measurement at ith ground station is represented as

$$az_{i,k} = \tan^{-1}\left(\frac{p_{y,k} - p_{y,gs_i}}{p_{x,k} - p_{x,gs_i}}\right) + \nu_{az_i}\,, \tag{38}$$

and the range rate at ith ground station is given by

$$\dot{r}_{i,k} = \frac{(p_{x,k} - p_{x,gs_i})v_{x,k} + (p_{y,k} - p_{y,gs_i})v_{y,k}}{\sqrt{(p_{x,k} - p_{x,gs_i})^2 + (p_{y,k} - p_{y,gs_i})^2}} + b_{i,k} + \nu_{\dot{r}_i}\,, \tag{39}$$

where ν_{r_i}, ν_{az_i} and $\nu_{\dot{r}_i}$ are discrete-time zero mean white Gaussian noises. p_{x,gs_i}, p_{y,gs_i} are the x-axis and y-axis coordinates of the ground station i. The bias $b_{i,k}$ is given by the following equation

$$\dot{b}_{i,k} = \tilde{\nu}_{b_i}\,, \tag{40}$$

which is different for different ground stations.

In Fig. 2a, the range, azimuth angle and rage rate measurements are shown from each ground station. The range rate biases of each ground station are depicted in Fig. 2b, which are different for different ground stations/nodes.

4.3. Augmented process model

In order to estimate the range rate bias, given by (40), we incorporate the bias dynamics in the process model. Thus, the augmented state vector becomes

$$\boldsymbol{x}_{i,k} = \begin{bmatrix} p_{x,k} & p_{y,k} & v_{x,k} & v_{y,k} & b_{i,k} \end{bmatrix}^T.$$

In discrete domain, the augmented state dynamics with sampling period ΔT is represented by

$$\boldsymbol{x}_{i,k+1} = \boldsymbol{A}_{i,k}\boldsymbol{x}_{i,k} + \boldsymbol{w}_{i,k}\,, \tag{41}$$

where

$$\boldsymbol{A}_{i,k} = \begin{bmatrix} \boldsymbol{A}_{\text{WNA}} & \boldsymbol{0}_{4\times 1} \\ \boldsymbol{0}_{4\times 1} & \boldsymbol{I}_{1\times 1} \end{bmatrix},\ \boldsymbol{A}_{\text{WNA}} = \begin{bmatrix} 1 & 0 & \Delta T & 0 \\ 0 & 1 & 0 & \Delta T \\ 0 & 0 & 1 & 0 \\ 0 & 0 & 0 & 1 \end{bmatrix}. \tag{42}$$

The continuous process noise vector $\tilde{\boldsymbol{w}}_{i,k}$ is given by

$$\tilde{\boldsymbol{w}}_k = [0 \quad 0 \quad \tilde{w}_x \quad \tilde{w}_y \quad \tilde{\nu}_{i,b}]^T.$$

and the covariance matrix $\boldsymbol{Q}_{i,k} = (E[\boldsymbol{w}_{i,k}\boldsymbol{w}_{i,k}^T])$ of discrete-time process noise $\boldsymbol{w}_{i,k}$ is represented as

$$\boldsymbol{Q}_{i,k} = \begin{bmatrix} \boldsymbol{Q}_{\text{WNA}} & \boldsymbol{0}_{4\times 1} \\ \boldsymbol{0}_{1\times 4} & \eta_b \Delta T \end{bmatrix}, \tag{43}$$

where

$$\boldsymbol{Q}_{\text{WNA}} = \begin{bmatrix} \eta_x \frac{\Delta T^3}{3} & 0 & \eta_x \frac{\Delta T^2}{2} & 0 \\ 0 & \eta_y \frac{\Delta T^3}{3} & 0 & \eta_y \frac{\Delta T^2}{2} \\ \eta_x \frac{\Delta T^2}{2} & 0 & \eta_x \Delta T & 0 \\ 0 & \eta_y \frac{\Delta T^2}{2} & 0 & \eta_y \Delta T \end{bmatrix}. \tag{44}$$

The above formulation of converting continuous time process noise to discrete time process noise and its error covariance estimation are explained in Bar-Shalom et al. [1]. The measurement matrix in (10) is given by

$$\boldsymbol{H}_{i,k} = \begin{bmatrix} \frac{\delta r}{\delta \boldsymbol{x}_i}\big|_{\boldsymbol{x}=\hat{\boldsymbol{x}}_{i,k|k-1}} \\ \frac{\delta az}{\delta \boldsymbol{x}_i}\big|_{\boldsymbol{x}=\hat{\boldsymbol{x}}_{i,k|k-1}} \\ \frac{\delta \dot{r}}{\delta \boldsymbol{x}_i}\big|_{\boldsymbol{x}=\hat{\boldsymbol{x}}_{i,k|k-1}} \end{bmatrix}. \tag{45}$$

The measurement noise vector and the measurement noise matrix are given by, respectively,

$$\boldsymbol{\nu}_{i,k} = [\nu_{r_{i,k}} \quad \nu_{az_{i,k}} \quad \nu_{\dot{r}_{i,k}}]^T, \quad \boldsymbol{R}_{i,k} = E[\boldsymbol{\nu}_{i,k}\boldsymbol{\nu}_{i,k}^T]. \tag{46}$$

In the DKF-NCS method, we divide the states into two state vectors (1.) common states and (2.) non-common states. The common states are the object related states, whereas non-common states are ground station specific. In this particular case, the commons state vector is $[p_x \quad p_y \quad v_x \quad v_y]^T$ and the non-common state vector is $[b_i]$.

4.4. Simulation results

In this subsection, simulation results of three different cases are presented. In the first case, described in Section 4.4.1, the simulation results are presented for no fault, i.e., the sensors are behaving according to their measurement model, and the initial state estimate is consistent with the initial error covariance matrix. In the second case, presented in Section 4.4.2, simulation results are shown for faulty measurements. In the third case, described in Section 4.4.3, simulation results are presented for incorrect initialization. In this simulation, the bias states are initialized with wrong values such that their estimation errors are not within $\pm 3\sigma$ bounds computed based on the initial error covariance, i.e., not consistent with the error covariance matrix. We evaluate the proposed algorithms on these three sets of simulations and compare with the χ^2 test based EDKF-NCS, where faulty measurements are isolated. Moreover, in Section 4.4.4, the proposed algorithms are compared with an adaptive extended Kalman filter (AEKF) presented in Mohamed and Schwarz [17] and their comparative analysis is also provided. These comparison studies with the χ^2 test

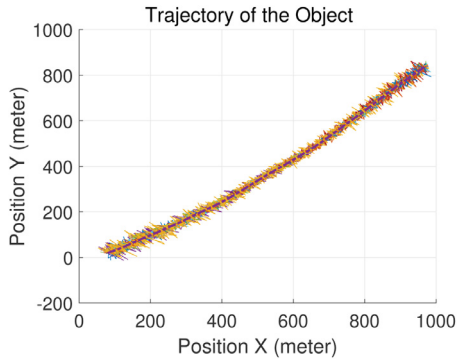

Fig. 3. Case 1: trajectory of the object with the measured range and azimuth angle.

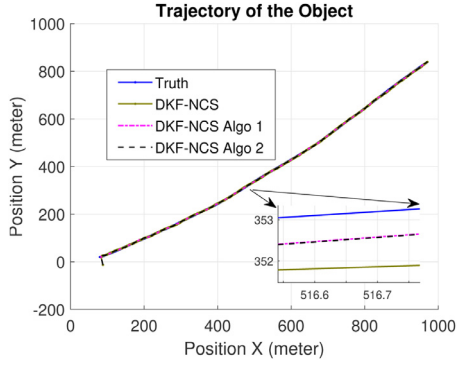

Fig. 4. Case 1: true and estimated trajectories of the object.

based EDKF-NCS as well as AEKF [17] demonstrate superiority of the proposed algorithms over these two existing methods.

We use the following conventions to describe the figures below. The EDKF-NCS with the χ^2 test is represented as 'DKF-NCS'. The adaptive EDKF-NCS using weighted correction is mentioned as 'DKF-NCS Algo-1', and the adaptive EDKF-NCS using measurement noise matrix modification is represented as 'DKF-NCS Algo-2'.

4.4.1. Case 1 - no fault

Simulation results are provided here for no fault, i.e., the measurement error is within the defined noise characteristics of the sensors. In Fig. 3, the measured trajectory is shown for each ground station using range and azimuth measurements by the following equations:

$$p_{x,k,meas} = r_{i,k}\cos(az_{i,k}) + p_{x,gs_i},$$
$$p_{y,k,meas} = r_{i,k}\sin(az_{i,k}) + p_{y,gs_i}.$$

As there are no faulty measurements, the performance of all three methods is expected to be the same. In Fig. 4, the true and estimated trajectories for DKF-NCS and the proposed two algorithms (DKF-NCS Algo-1 and DKF-NCS Algo-2) are shown. It can be seen from this figure that estimated trajectories are close to the truth trajectory. Also, the estimated trajectories are less noisy compared to the measured trajectories in Fig. 3. In Fig. 5, the position estimation errors are depicted mostly within their $\pm 3\sigma$ bounds for all the three algorithms. The position estimation errors are similar for DKF-NCS, DKF-NCS Algo-1 and DKF-NCS Algo-2.

Fig. 6 represents the true range rate biases and the estimated range rate biases for the proposed methods and DKF-NCS of ground station 1. It can be seen from the top subplot of this figure that the estimated range rate biases are close to the true range rate biases. The estimation errors in range rate biases for all the filters are within $\pm 3\sigma$ bounds, as shown in the bottom subplot of the

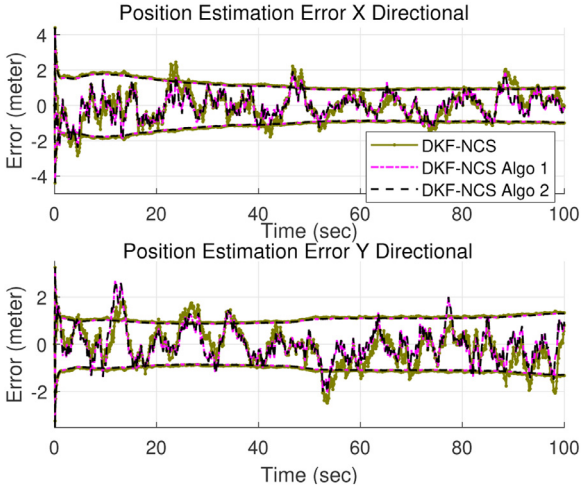

Fig. 5. Case 1: position estimation error.

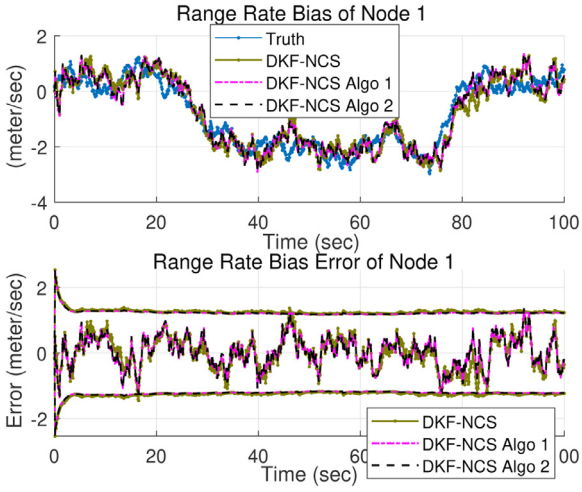

Fig. 6. Case 1: range rate bias estimates of ground station 1.

figure. The range rate bias estimation errors are almost the same for all three algorithms.

In Fig. 7, the cumulative distribution function (CDF) plots of position and velocity estimation errors are presented for 100 simulation runs. The averaged root-mean-square (RMS) estimation errors of position and velocity per run are used to generate the CDF plots. From these two figures, it can be confirmed that the proposed two adaptive DKF-NCS algorithms are slightly better than the DKF-NCS (χ^2 test) for no fault case.

4.4.2. Case 2 - faulty measurements

In this case, simulation results are provided for faulty measurements. To introduce fault in measurements, biases are added to the measurements randomly in one of the ground station measurements. The trajectories generated from the range and azimuth measurements for this case study are shown in Fig. 8 for all the ground stations. As it can be seen that the generated trajectories are noisier in comparison with the trajectories generated from the normal measurements, depicted in Fig. 3.

Once the measurements are generated, the same measurements are fed to the DKF-NCS and adaptive DKF-NCS estimators. The position estimation errors along with their $\pm 3\sigma$ bounds are shown in Fig. 9. From these figures, it is observed that the performance of DKF-NCS Algo-1 and DKF-NCS Algo-2 is comparatively better than the χ^2 distribution based DKF-NCS method for the run.

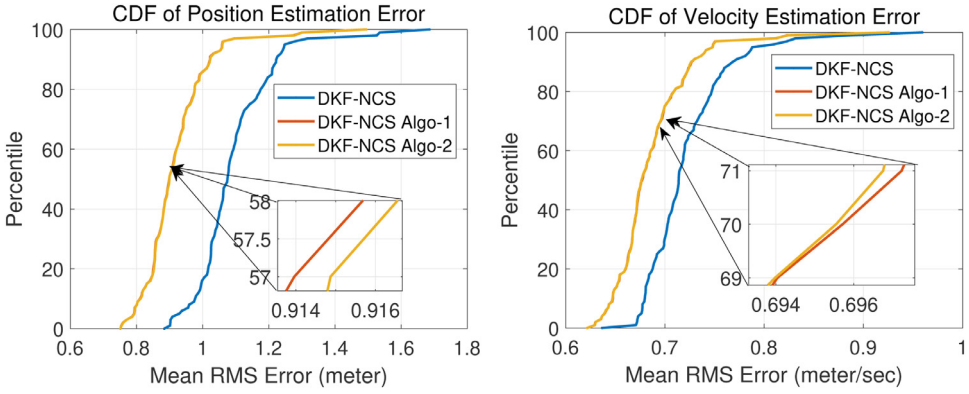

Fig. 7. Case 1: CDF of position and velocity estimation errors for 100 runs.

Fig. 8. Case 2: trajectory of the object with the measured range and azimuth angle.

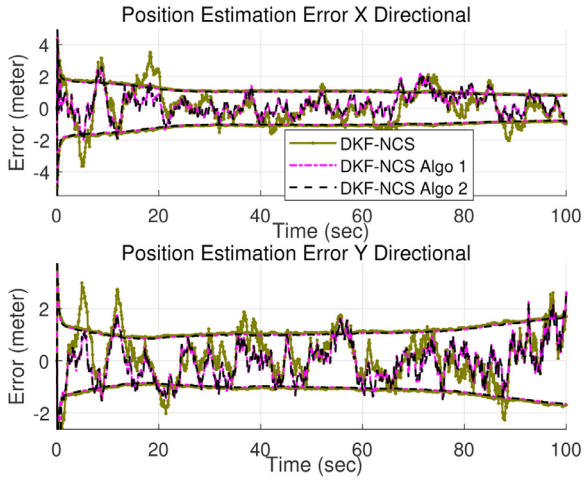

Fig. 9. Position estimation error.

Fig. 10 shows the true range rate bias and estimated range rate biases from three methods for ground station 1. The estimation errors for all three methods are shown in the figure. It can be seen from this figure that the estimates for three methods are mostly close to the true values, as well as the estimation errors are within by $\pm 3\sigma$ bounds most of the time and are almost the same for three methods.

The CDF plots for three methods are depicted for 100 simulation runs in Fig. 11. It can be observed that the proposed two adaptive DKF-NCS methods are slightly better than the χ^2 distribution based DKF-NCS method, when faulty measurements are processed by the estimators.

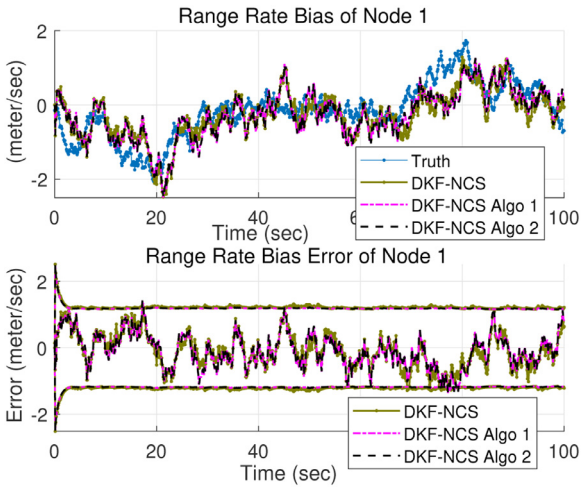

Fig. 10. Range rate bias estimates of ground station 1.

4.4.3. Case 3 - incorrect initialization

In the third set of simulations, the bias states are initialized with wrong values deliberately. The initialization is same for all three methods.

The position estimation errors with $\pm 3\sigma$ bounds are shown in Fig. 12. It can be noted that the position estimation error for DKF-NCS is higher than that of the proposed two adaptive DKF-NCS.

In Fig. 13, the range rate bias estimates and the true range rate bias are shown. The estimates of all three filters are initialized with wrong values such that their estimation errors are not covered by $\pm 3\sigma$ bounds computed based on the initial error covariance, as shown in this figure. The range rate bias estimate converges faster for the proposed two adaptive methods compared to DKF-NCS. The incorrect initialization of range rate bias causes performance issue as shown in the position estimation error plot in Fig. 12. The estimation error in the DKF-NCS is the highest among the three estimators. Due to wrong initial value of range rate bias, the predicted state estimates and predicted measurements are incorrect and not covered by their $\pm 3\sigma$ bounds. Therefore, all the good measurements get isolated by χ^2 test. But, in the case of the proposed adaptive DKF-NCS methods, the measurements are used with less weights. Thus, DKF-NCS Algo-1 and DKF-NCS Algo-2 converge faster than DKF-NCS.

In Fig. 14, the CDF plots for position and velocity estimation errors are depicted for 100 simulation runs. From the figures, it is evident that the proposed two adaptive DKF-NCS perform equally well, but much better than the DKF-NCS.

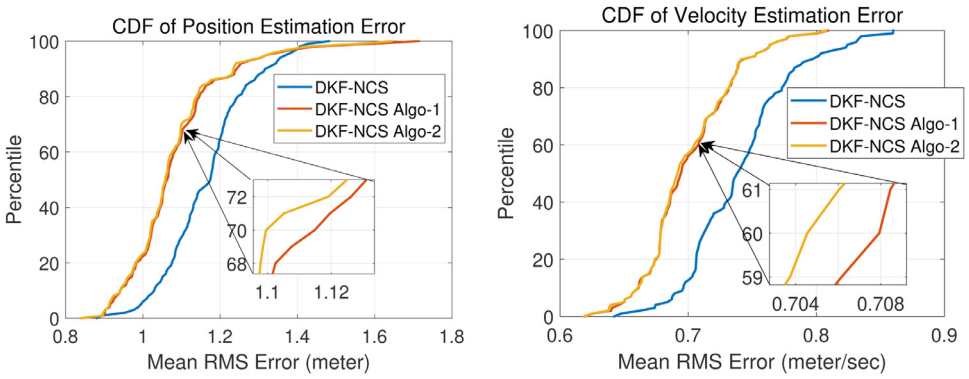

Fig. 11. Case 2: CDF of position and velocity estimation errors for 100 runs.

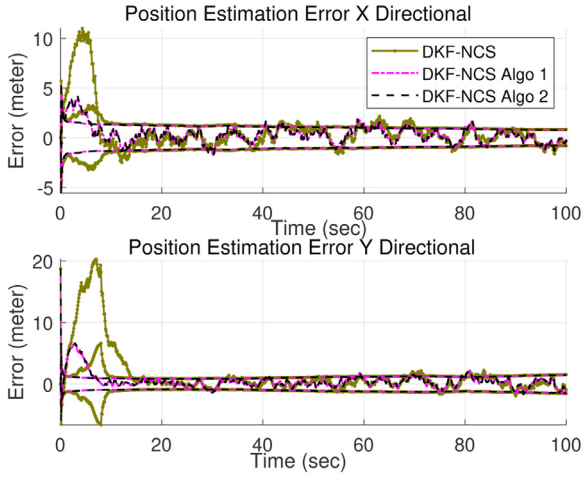

Fig. 12. Case 3: position estimation error.

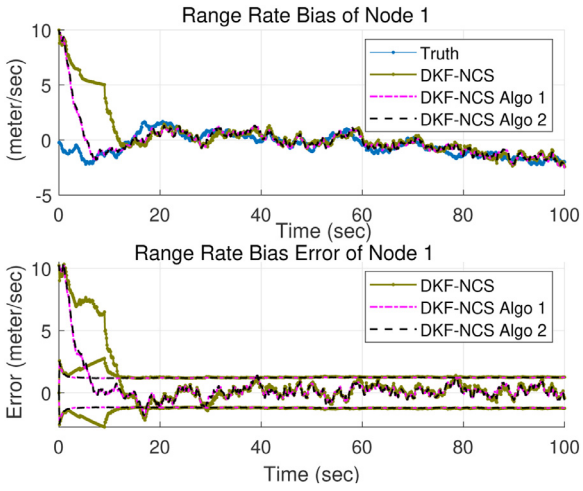

Fig. 13. Case 3: range rate bias estimates of ground station 1.

From Figs. 7, 11 and 14, it is clear that the performance of the proposed two adaptive methods is consistent in all three cases, whereas DKF-NCS does not perform well especially in Case 3 - incorrect bias initialization.

4.4.4. Comparison with adaptive extended Kalman filter [17]

In this subsection, a comparative study of the proposed algorithms with respect to the adaptive extended Kalman filter (AEKF) [17] is provided. The initial value of error covariance matrix as well as process and measurement noise matrices for AEKF are selected as the same as those for the proposed methods. Also, a sliding history window of immediate previous 10 residuals at each time is chosen for AEKF. The plots of position and velocity estimation errors for AEKF are not shown here, as these estimation error plots for a single run are similar to the plots shown earlier in Sections 4.4.1–4.4.3, and in order to limit the length of the paper. However, the CDF plots are depicted for mean RMS position estimation error and velocity estimation error for 100 simulation runs. The CDF plots are presented for three different cases, as discussed in the previous sections, (i) Case 1 - No Fault, (ii) Case 2 - Faulty Measurements, (iii) Case 3 - Incorrect Initialization.

In Fig. 15, the CDF plots are shown for Case 1, when there is no fault, i.e., measurements are consistent with the measurement

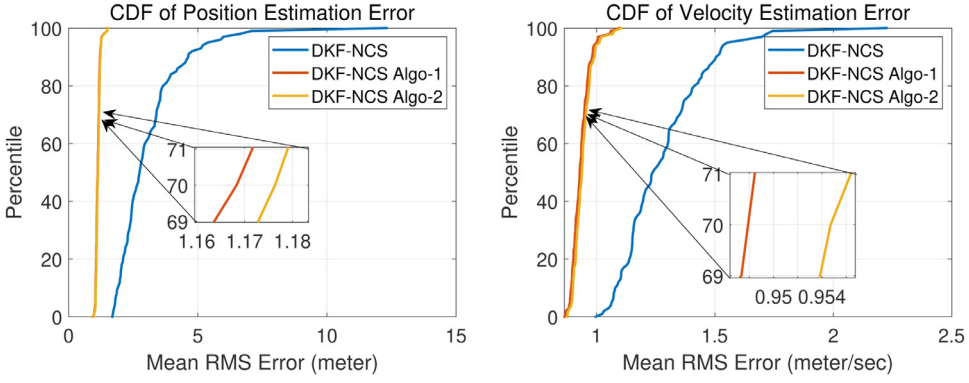

Fig. 14. Case 3: CDF of position and velocity estimation errors for 100 runs.

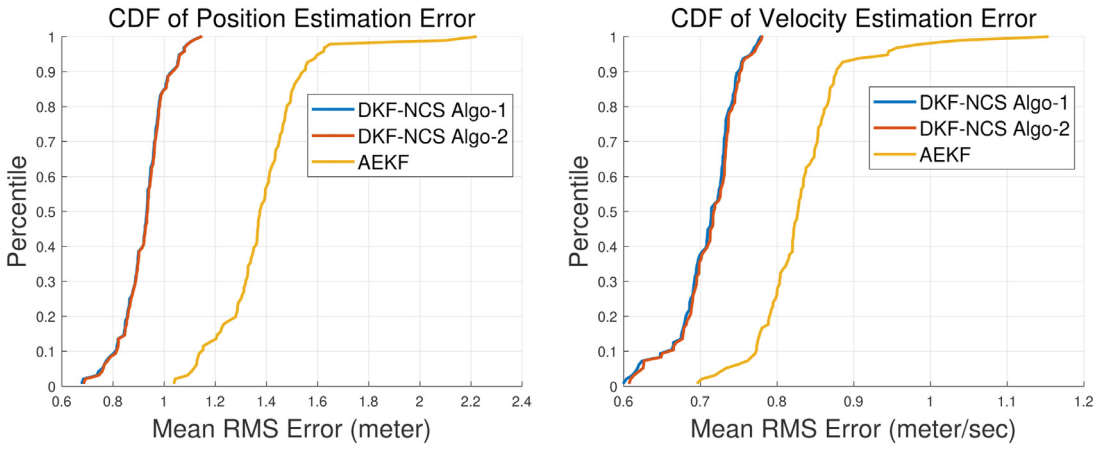

Fig. 15. Comparison with AEKF - Case 1: CDF of position and velocity estimation errors for 100 runs.

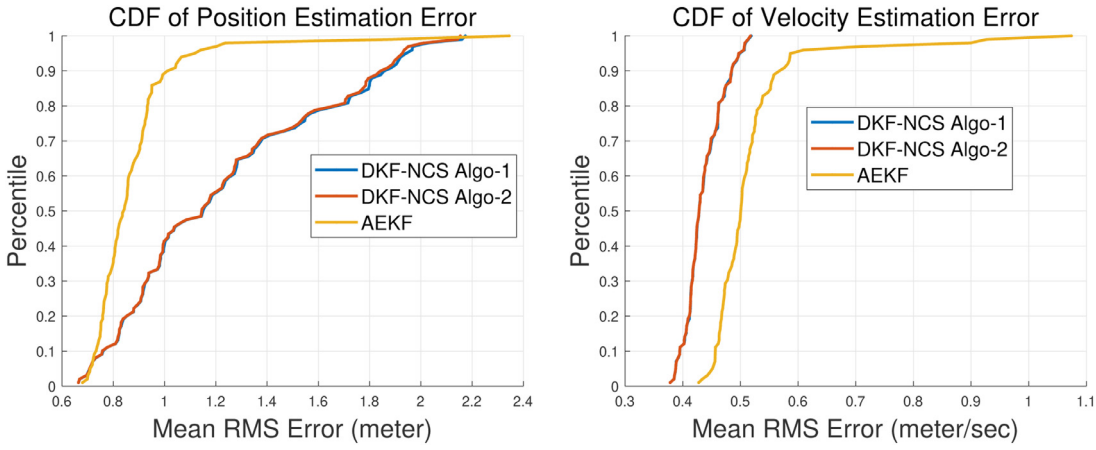

Fig. 16. Comparison with AEKF - Case 2: CDF of position and velocity estimation errors for 100 runs.

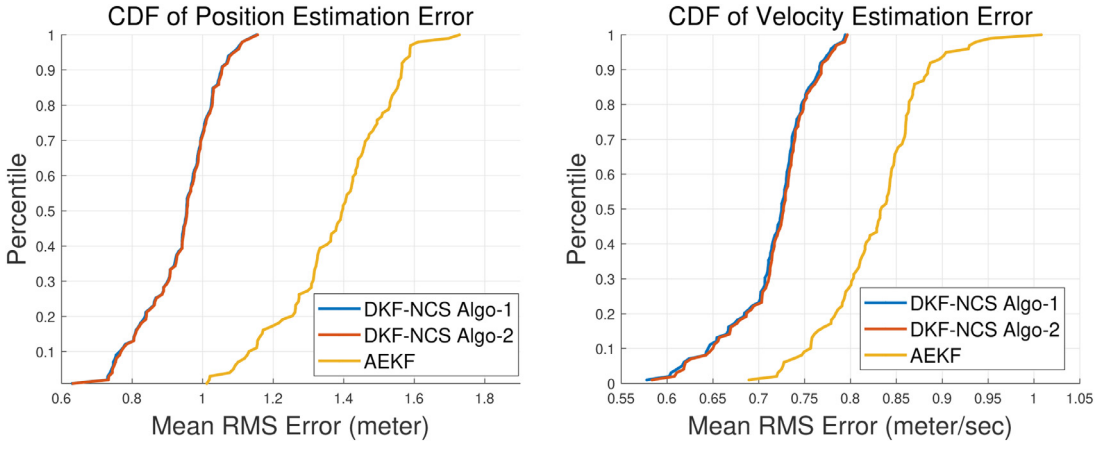

Fig. 17. Comparison with AEKF - Case 3: CDF of Position and Velocity Estimation Errors for 100 Runs.

noise matrix. It can be observed that both the proposed methods work better than AEKF. Since this is no fault simulation and AEKF uses history of residuals to compute adaptive measurement noise matrix, the performance of AEKF is slightly degraded as adaptive measurement noise matrix of AEKF does not truly represent the actual measurement noise matrix.

In Fig. 16, the CDF plots are depicted for Case 2, where the measurements are faulty, i.e., measurements are not consistent with the measurement noise matrix. Since the residuals represent the true error in the measurements as the predicted measurements are consistent with the predicted measurement error covariance matrix, therefore, the computed measurement noise matrix is close to the actual measurement noise matrix. Hence, the CDF plot for position estimation error is better for AEKF. However, the CDF plots for velocity estimation error are better for the proposed methods. This is because the faults are introduced in the range and angle measurements, but not in the range rate measurements.

In Fig. 17, the CDF plots for Case 3 are shown, where the bias states are initialized incorrectly, i.e., measurements are consistent with the measurement noise matrix, but the predicted measure-

ments are not consistent with the predicted measurement noise matrix. In such a scenario, the proposed methods show better performance than AEKF, as seen in the figure. In this case, adaptive measurement noise matrix of AEKF does not represent the true measurement noise matrix due to incorrect residual computation. The residuals are incorrect due to the fact that the bias states are initialized incorrectly and cause inconsistent measurement prediction. Therefore, the performance of AEKF is degraded compared to that of the proposed methods.

In most of the cases, it is evident from Figs. 15–17 that the proposed methods show lower estimation errors compared to AEKF.

Remark 6. The simulation results of Case 3 are presented for incorrect bias state initialization. The objective of Case 3 simulations is to show that the inconsistency in predicted state estimate and its error covariance matrix can cause corrected state estimate to diverge from its true value due to wrongly isolating valid measurements. In Case 3 simulations, this inconsistency arises due to incorrect bias state initialization. The same inconsistency is observed, if previous state estimate is not consistent with its error covariance matrix or the control input is wrong.

5. Conclusion and future work

In this paper, two adaptive decentralized Kalman filters with non-common states for nonlinear systems have been presented to handle fault in measurements. The first algorithm has handled faulty measurements at the assimilation step by applying weighted correction. The second algorithm has modified the measurement noise matrix based on a closed-form solution, if there is any fault. Using 100 simulation runs, the proposed methods have been compared with the extended decentralized Kalman filter with non-common states, which employs the χ^2 distribution test to detect and isolate the measurements, and an existing adaptive extended Kalman filter, for a target tracking problem. Three different cases have been evaluated to validate the performance of the proposed algorithms. In most of the cases, the proposed methods have performed well compared to these two existing methods.

In this paper, the χ^2 distribution based method has been used to compute the weighting factor α. There could be other ways to make α more adaptive, which can be an interesting future research direction.

Declaration of Competing Interest

Authors declare that they have no conflict of interest.

References

[1] Y. Bar-Shalom, X.R. Li, T. Kirubarajan, Estimation with Applications to Tracking and Navigation: Theory Algorithms and Software, John Wiley & Sons, 2004, pp. 234–236, doi:10.1002/0471221279. 273–274

[2] R. Da, C.-F. Lin, Sensor failure detection with a bank of Kalman filters, in: Proceedings of American Control Conference, 2, IEEE, Seattle, WA, USA, 1995, pp. 1122–1126, doi:10.1109/ACC.1995.520920.

[3] Z. Gao, C. Cecati, S.X. Ding, A survey of fault diagnosis and fault-tolerant techniques—Part I: fault diagnosis with model-based and signal-based approaches, IEEE Trans. Ind. Electron. 62 (6) (2015) 3757–3767, doi:10.1109/TIE.2015.2417501.

[4] P.D. Hanlon, P.S. Maybeck, Characterization of Kalman filter residuals in the presence of mismodeling, IEEE Trans. Aerosp. Electron. Syst. 36 (1) (2000a) 114–131, doi:10.1109/7.826316.

[5] P.D. Hanlon, P.S. Maybeck, Multiple-model adaptive estimation using a residual correlation Kalman filter bank, IEEE Trans. Aerosp. Electron. Syst. 36 (2) (2000b) 393–406, doi:10.1109/7.845216.

[6] I. Hwang, S. Kim, Y. Kim, C.E. Seah, A survey of fault detection, isolation, and reconfiguration methods, IEEE Trans. Control Syst. Technol. 18 (3) (2010) 636–653, doi:10.1109/TCST.2009.2026285.

[7] A. Izadian, Self-tuning fault diagnosis of MEMS, Mechatronics 23 (8) (2013) 1094–1099, doi:10.1016/j.mechatronics.2013.08.006.

[8] M. Kazemi, M. Karrari, M. Menhaj, A new class of decentralized estimators for large-scale systems, Eur. J. Control 9 (5) (2003) 474–482, doi:10.3166/ejc.9.474-482.

[9] J.-Y. Keller, A fault detection filter including an adaptive noise cancellation strategy, Eur. J. Control 13 (6) (2007) 627–638, doi:10.3166/ejc.13.627-638.

[10] P.J. Lawrence, M.P. Berarducci, Comparison of federated and centralized Kalman filters with fault detection considerations, in: Proceedings of 1994 IEEE Position, Location and Navigation Symposium, IEEE, Las Vegas, NV, USA, 1994, pp. 703–710, doi:10.1109/PLANS.1994.303380.

[11] P. Li, F. Boem, G. Pin, Fast-convergent fault detection and isolation in a class of nonlinear uncertain systems, Eur. J. Control 55 (2020) 45–55, doi:10.1016/j.ejcon.2020.05.011.

[12] P. Lu, L. Van Eykeren, E. van Kampen, Q.P. Chu, Selective-reinitialization multiple-model adaptive estimation for fault detection and diagnosis, J. Guid., Control, Dyn. 38 (8) (2015) 1409–1424, doi:10.2514/1.G000587.

[13] P.S. Maybeck, Multiple model adaptive algorithms for detecting and compensating sensor and actuator/surface failures in aircraft flight control systems, Int. J. Robust Nonlinear Control 9 (14) (1999) 1051–1070, doi:10.1002/(SICI)1099-1239(19991215)9:14<1051::AID-RNC452)3.0.CO;2-0.

[14] P.S. Maybeck, P.D. Hanlon, Performance enhancement of a multiple model adaptive estimator, in: Proceedings of 32nd IEEE Conference on Decision and Control, 1, IEEE, San Antonio, TX, USA, 1993, pp. 462–468, doi:10.1109/CDC.1993.325104.

[15] R.K. Mehra, J. Peschon, An innovations approach to fault detection and diagnosis in dynamic systems, Automatica 7 (5) (1971) 637–640, doi:10.1016/0005-1098(71)90028-8.

[16] T.E. Menke, P.S. Maybeck, Sensor/actuator failure detection in the vista F-16 by multiple model adaptive estimation, IEEE Trans. Aerosp. Electron. Syst. 31 (4) (1995) 1218–1229, doi:10.1109/7.464346.

[17] A.H. Mohamed, K.P. Schwarz, Adaptive Kalman filtering for INS/GPS, J. Geodesy 73 (4) (1999) 193–203, doi:10.1007/s001900050236.

[18] K. Neema, D.A. DeLaurentis, Distributed fault detection and isolation for Kalman consensus filter, in: AIAA Guidance, Navigation, and Control (GNC) Conference, AIAA, 2013, doi:10.2514/6.2013-4948. AIAA 2013–4948

[19] B.S.Y. Rao, H.F. Durrant-Whyte, J.A. Sheen, A fully decentralized multi-sensor system for tracking and surveillance, Int. J. Robot. Res. 12 (1) (1993) 20–44, doi:10.1177/027836499301200102.

[20] X.-X. Ren, G.-H. Yang, Kullback–Leibler divergence-based optimal stealthy sensor attack against networked linear quadratic gaussian systems, IEEE Trans. Cybern. (2021a) 1–10, doi:10.1109/TCYB.2021.3068220.

[21] X.-X. Ren, G.-H. Yang, Noise covariance estimation for networked linear systems under random access protocol scheduling, Neurocomputing 455 (2021b) 68–77, doi:10.1016/j.neucom.2021.05.052.

[22] V. Saini, A. Maity, Extended decentralized Kalman filter with non-common states and its stochastic stability, Under Rev. J. (2021) 1–12.

[23] V. Saini, A.A. Paranjape, A. Maity, Decentralized information filter with non-common states, J. Guid., Control, Dyn. 42 (9) (2019) 2042–2054, doi:10.2514/1.G003862.

[24] V.K. Saini, A. Maity, Weighted adaptive decentralized Kalman filters for fault tolerance, in: AIAA Scitech Forum, AIAA, 2020, doi:10.2514/6.2020-0949. AIAA 2020-0949

[25] D. Simon, D.L. Simon, Kalman filter constraint switching for turbofan engine health estimation, Eur. J. Control 12 (3) (2006) 331–343, doi:10.3166/ejc.12.341-343.

[26] H.E. Soken, C. Hajiyev, S. ichiro Sakai, Robust Kalman filtering for small satellite attitude estimation in the presence of measurement faults, Eur. J. Control 20 (2) (2014) 64–72, doi:10.1016/j.ejcon.2013.12.002.

[27] J.L. Speyer, Computation and transmission requirements for a decentralized linear-quadratic-gaussian control problem, IEEE Trans. Autom. Control 24 (2) (1979) 266–269, doi:10.1109/TAC.1979.1101973.

[28] L. Summerer, J. Keller, M. Darouach, Robust fault diagnosis with a two-stage Kalman estimator, Eur. J. Control 3 (3) (1997) 247–252, doi:10.1016/S0947-3580(97)70082-7.

[29] J.V. Tsyganova, M.V. Kulikova, A.V. Tsyganov, A general approach for designing the MWGS-based information-form Kalman filtering methods, Eur. J. Control 56 (2020) 86–97, doi:10.1016/j.ejcon.2020.02.001.

[30] N.A. White, P.S. Maybeck, S.L. DeVilbiss, Detection of interference/jamming and spoofing in a DGPS-aided inertial system, IEEE Trans. Aerosp. Electron. Syst. 34 (4) (1998) 1208–1217, doi:10.1109/7.722708.

[31] Y. Xia, W. Yang, Z. Zhao, Consensus-based filtering under false data injection attacks, Eur. J. Control 48 (2019) 3–8, doi:10.1016/j.ejcon.2018.11.004.